





# The rice OsERF101 transcription factor regulates the NLR Xa1-mediated immunity induced by perception of TAL effectors

Ayaka Yoshihisa<sup>1\*</sup>, Satomi Yoshimura<sup>1\*</sup>, Motoki Shimizu<sup>2</sup> , Sayaka Sato<sup>1</sup>, Shogo Matsuno<sup>1</sup>, Akira Mine<sup>3</sup> ,  
Koiji Yamaguchi<sup>1</sup>  and Tsutomu Kawasaki<sup>1,4</sup> 

<sup>1</sup>Department of Advanced Bioscience, Graduate School of Agriculture, Kindai University, Nakamachi, Nara 631-8505, Japan; <sup>2</sup>Division of Genomics and Breeding, Iwate Biotechnology Research Center, Iwate 024-0003, Japan; <sup>3</sup>Graduate School of Agriculture, Kyoto University, Kyoto 606-8502, Japan; <sup>4</sup>Agricultural Technology and Innovation Research Institute, Kindai University, Nakamachi, Nara 631-8505, Japan

## Summary

Author for correspondence:  
Tsutomu Kawasaki  
Email: t-kawasaki@nara.kindai.ac.jp

Received: 31 August 2021  
Accepted: 8 August 2022

New Phytologist (2022) 236: 1441–1454  
doi: 10.1111/nph.18439

**Key words:** immunity, nucleotide-binding leucine-rich repeat receptors (NLRs), rice, transcription activator-like (TAL) effector, *Xanthomonas*.

- Plant nucleotide-binding leucine-rich repeat receptors (NLRs) initiate immune responses by recognizing pathogen effectors. The rice gene *Xa1* encodes an NLR with an N-terminal BED domain, and recognizes transcription activator-like (TAL) effectors of *Xanthomonas oryzae* pv *oryzae* (*Xoo*). Our goal here was to elucidate the molecular mechanisms controlling the induction of immunity by *Xa1*.
- We used yeast two-hybrid assays to screen for host factors that interact with *Xa1* and identified the AP2/ERF-type transcription factor OsERF101/OsRAP2.6. Molecular complementation assays were used to confirm the interactions among *Xa1*, OsERF101 and two TAL effectors. We created *OsERF101*-overexpressing and knockout mutant lines in rice and identified genes differentially regulated in these lines, many of which are predicted to be involved in the regulation of response to stimulus.
- *Xa1* interacts in the nucleus with the TAL effectors and OsERF101 via the BED domain. Unexpectedly, both the overexpression and the knockout lines of *OsERF101* displayed *Xa1*-dependent, enhanced resistance to an incompatible *Xoo* strain. Different sets of genes were up- or downregulated in the overexpression and knockout lines.
- Our results indicate that OsERF101 regulates the recognition of TAL effectors by *Xa1*, and functions as a positive regulator of *Xa1*-mediated immunity. Furthermore, an additional *Xa1*-mediated immune pathway is negatively regulated by OsERF101.

## Introduction

Plants have developed two tiers of immune systems to defend against pathogen infection. The first tier is initiated through recognition of microbe-associated molecular patterns by plasma membrane-localized pattern recognition receptors. This is referred to as pattern-triggered immunity (Dangl *et al.*, 2013). To inhibit pattern-triggered immunity or to improve the nutrient conditions suitable for pathogen proliferation, pathogens deliver a variety of effectors into plant cells (Dou & Zhou, 2012). For the second tier of immune responses, plants have evolved a family of nucleotide-binding (NB) leucine-rich repeat (LRR) receptors (NLRs) that directly or indirectly recognize pathogen effectors (Jones *et al.*, 2016). This is referred to as effector-triggered immunity. Effector-triggered immunity often involves a hypersensitive cell death response (HR). Several NLRs indirectly recognize pathogen effectors by interacting with host factors. These host factors are defined as ‘sensing decoys’ that mimic the targets of

pathogen effectors and act as coreceptors with the NLRs (van der Hoorn & Kamoun, 2008; Paulus & van der Hoorn, 2018).

*Xanthomonas oryzae* pv *oryzae* (*Xoo*) causes rice bacterial blight disease, one of the most important rice diseases in the world. *Xoo* has developed transcription-activator-like (TAL) effectors to facilitate bacterial growth. Transcription activator-like effectors contain a central region of polymorphic repeats (central repeat region, CRR) with each repeat consisting of 34 amino acid residues, several nuclear localization signals (NLSs) and an activation domain at the C terminus. Each of the repeats in the CRR specifies a nucleotide for binding (Boch *et al.*, 2009; Moscou & Bogdanove, 2009). *Xoo* secretes TAL effectors into rice cells through a type III secretion system, and the TAL effectors then localize to the host nuclei to regulate expression of certain host genes. One of the *Xoo* TAL effectors, AvrXa7, accelerates expression of the *SWEET14* gene, which encodes a plasma membrane-localized sugar transporter (Antony *et al.*, 2010). The enhanced accumulation of SWEET14 protein increases the efflux of sugars from the cytoplasm to the apoplast, and this provides additional nutrients for the pathogen (Naseem *et al.*, 2017). This process is very

\*These authors contributed equally to this work as first coauthors.

important for bacterial virulence, because defects in the expression of *SWEET14* greatly reduce bacterial growth (Oliva *et al.*, 2019).

The bacterial blight disease resistance gene *Xa1* was identified originally in the rice cultivar Kogyoku (Yoshimura *et al.*, 1998). It encodes an NLR protein with an N-terminal BED-type zinc finger domain. *Xa1* recognizes TAL effectors and induces immune responses including the HR (Ji *et al.*, 2016), but the mechanisms for these processes have not been elucidated. Recently, alleles of *Xa1* called *Xa2*, *Xa14*, *Xa45* and *Xo1* have been isolated (Ji *et al.*, 2020; Read *et al.*, 2020; Zhang *et al.*, 2020). Their predicted protein structures indicate that the BED and NB regions are highly conserved, but their C-terminal LRR regions are distinguished by the number of repeats. This suggests that the LRR regions may determine the interactions with TAL effectors (Read *et al.*, 2020).

The immune responses induced when *Xa1* and its allelic NLR proteins recognize TAL effectors can be suppressed by interfering TAL (iTAL) effectors, also referred to as truncated TAL (trunc-TAL) effectors (Ji *et al.*, 2016, 2020; Read *et al.*, 2016). iTAL effectors lack the activation domain but retain the NLSs. iTAL effectors can be classified into two types (A and B) based on their structures (Ji *et al.*, 2016; Read *et al.*, 2016). However, the molecular mechanisms by which iTAL effectors suppress *Xa1*-mediated immunity remain to be revealed.

In this study, we found that the BED domain of *Xa1* forms a complex with two TAL effectors, *AvrXa7* and *Xoo1132*. To understand the molecular mechanism of *Xa1*-mediated immunity, we screened for proteins that interact with *Xa1*, and identified *OsERF101/OsRAP2.6*, a member of the AP2/ERF-type family of transcription factors. We investigated the interactions between *OsERF101* and *Xa1* in plants. We also analyzed *Xa1*-dependent resistance and TAL effector-induced gene expression using plants that overexpressed *OsERF101* and plants carrying knockout mutations of *OsERF101*. Furthermore, we found that *OsERF101* directly interacts with the TAL effectors. The results of these experiments suggest that *OsERF101* is probably involved in both effector recognition and immune activation mediated by *Xa1*.

## Materials and Methods

### Plant materials

Rice (*Oryza sativa*) *Japonicum* cultivars Kogyoku and Nipponbare were used as the wild-type plants. The *xa1* and *oserf101* mutants were generated using the CRISPR/Cas9 system as described below. The *OsERF101*-OX plants were generated as described below.

### Plant transformation

To construct the plasmids for the CRISPR/Cas9 system, we used the guide RNA cloning vector pU6gRNA and the all-in-one Cas9/gRNA vector pZDgRNA\_Cas9ver.2\_HPT, which were kindly provided by Dr Masaki Endo (Mikami *et al.*, 2015). The

20 bp sequences from 108 to +127 of *Xa1* (5'-GCAACTGGTCTGCAAAGATC-3') and from 206 to +225 of *OsERF101* (5'-GTGTTTCGACAGCGGCCATGG-3') were selected as the target sites of Cas9 by using the CRISPR-P website (<http://cbi.hzau.edu.cn/cgi-bin/CRISPR>). These DNA fragments were cloned into pU6gRNA, and then subcloned into pZDgRNA\_Cas9ver.2\_HPT (Mikami *et al.*, 2015). Calli generated from rice embryos were transformed using *Agrobacterium tumefaciens* EHA101 carrying each construct, as described previously (Hiei *et al.*, 1994). To confirm the mutations, the genomic regions containing the Cas9 target sites were amplified by PCR and sequenced as previously described (Mikami *et al.*, 2015). For overexpression, the entire coding region of *OsERF101* was amplified with gene-specific primers (Supporting Information Table S1) using cDNAs prepared from cv Kogyoku leaves as the templates, and the PCR product was cloned into the binary vector pGWB2 (Nakagawa *et al.*, 2007). In the resulting construct, the *OsERF101* gene was driven by the CaMV 35S promoter. Calli generated from rice embryos were transformed with the construct as described previously (Hiei *et al.*, 1994).

### Transient assays using rice protoplasts

Protoplasts were isolated from cultured rice cells by digestion of the cell walls with Cellulase RS (Yakult Pharmaceutical, Tokyo, Japan) and Macerozyme R-10 (Yakult Pharmaceutical) as described previously (Yamaguchi *et al.*, 2013). Aliquots (100  $\mu$ l) of protoplasts ( $2.5 \times 10^6$  cells  $\text{ml}^{-1}$ ) were transformed with plasmid DNA using the polyethylene glycol (PEG) method (Chen *et al.*, 2010). For subcellular localization analysis and bimolecular fluorescence complementation (BiFC) analysis, transfected protoplasts were observed using a fluorescence microscope, the Axio Imager M2 (Carl Zeiss, Oberkochen, Germany) with the Apo-Tome2 system (Carl Zeiss). The BiFC analyses were carried out as reported previously (Yamaguchi *et al.*, 2013).

### Split NanoLuc luciferase complementation assay

DNA fragments of *Xa1*<sup>1-1802</sup>, *Xa1*<sup>1-325</sup>, *Xa1*<sup>312-1012</sup>, *Xa1*<sup>1008-1802</sup>, *AvrXa7* and *Xoo1132* were transferred into *p35S-GW-T7-LgBiT*, *p35S-GW-T7-SmBiT* or *p35S-SmBiT-GW-T7* using the Gateway system with LR clonase reactions (Taoka *et al.*, 2021). The Firefly *Luciferase* gene controlled by the CaMV 35S promoter was used as an internal control. The constructs were transfected into rice protoplasts as described above. After 18 h of incubation at 30°C, activities of the Firefly and NanoLuc luciferases were measured in a TriStar2 LB942 luminometer (Berthold, Bad Wildbad, Germany) using the ONE-Glo Luciferase Assay System (Promega, Madison, WI, USA) and the Nano-Glo Live Cell Assay System (Promega).

### Yeast two-hybrid assays

The yeast two-hybrid screening and interaction assays were based on the requirement for histidine for yeast growth, as described previously (Ishikawa *et al.*, 2014).

## Protein extraction and immunoblotting

Total proteins were extracted from rice protoplasts in a buffer including 50 mM Tris-HCl pH 7.5, 1 mM EDTA, and a protease inhibitor cocktail (Roche), and analyzed by immunoblotting with  $\alpha$ -HA,  $\alpha$ -Lg and  $\alpha$ -T7.

## Pathology assays

Fully expanded rice leaves were inoculated with *Xoo* T7174 or *Xoo* T7133 by infiltration of the bacterial suspension (OD<sub>600</sub> = 0.25) with a needleless syringe. The bacterial populations in the leaves after infiltration were analyzed by quantitative real-time PCR. The DNA levels of the *Xoo XopA* gene relative to those of the rice *ubiquitin* gene were measured using genomic DNAs purified from the infected leaves.

## RNA isolation and quantitative real-time PCR

Total RNA was isolated from rice leaves using TRIzol reagent (Invitrogen, Carlsbad, CA, USA) and then treated with RNase-free DNase I (Roche). First-strand cDNA was synthesized from 1  $\mu$ g total RNA using an oligo-dT primer and ReverTra Ace reverse transcriptase (Toyobo, Osaka, Japan). Expression levels were measured by quantitative real-time PCR using the SYBR Green master mix (Applied Biosystems, Foster City, CA, USA) in a Step-One Plus Real-Time PCR system (Applied Biosystems). The expression levels were normalized against a *ubiquitin* reference gene. Three biological replicates were used for each experiment, and two quantitative replicates were performed for each biological replicate.

## RNA-sequencing

Total RNA was used to make sequencing libraries using a NEBNext Ultra RNA Library Prep Kit for Illumina (NEB, Ipswich, MA, USA) according to the manufacturer's instructions. Subsequently, the libraries were sequenced using an Illumina HiSeq4000 platform to obtain 150 bp paired-end reads, and the RNA-sequencing (RNA-seq) data were deposited in the DNA Databank of Japan (DDBJ) under the BioProject accession no. PRJDB13649. FAQCS (Lo & Chain, 2014) software was used to filter high-quality reads from the generated sequence reads. The filtered reads were aligned with the rice reference sequence for cv Nipponbare ([http://rice.plantbiology.msu.edu/pub/data/Eukaryotic\\_Projects/o\\_sativa/annotation\\_dbs/pseudomolecules/version\\_7.0/all.dir/all.con](http://rice.plantbiology.msu.edu/pub/data/Eukaryotic_Projects/o_sativa/annotation_dbs/pseudomolecules/version_7.0/all.dir/all.con)) using HISAT2 (Kim *et al.*, 2015) software, and counted for each gene using FEATURECOUNTS (Liao *et al.*, 2014) software. Differentially expressed genes (DEGs) were detected using a TCC package (Sun *et al.*, 2013). The enrichment analysis of *cis* regulatory elements was carried out using the Analysis of Motif Enrichment tool of the MEME suite of motif databases (<https://meme-suite.org/meme/tools/ame>). Gene Ontology (GO) analysis of the DEGs was performed using RICE NETDB (<http://bis.zju.edu.cn/ricenetdb/>).

## Results

### Xa1 interacts with TAL effectors in the rice nucleus

To analyze the interactions between Xa1 and TAL effectors, we first used Xa1 protein fusions with green fluorescence protein (GFP) to determine their subcellular localization in transiently expressing rice protoplasts. Green fluorescence protein was fused to the N termini of full-length Xa1<sup>1–1802</sup> and three different Xa1 regions: Xa1<sup>1–325</sup>, Xa1<sup>312–1012</sup> and Xa1<sup>1008–1802</sup>. These three regions contained the BED, NB and LRR domains, respectively (Fig. 1a). GFP-Xa1<sup>1–325</sup> was localized mainly in the nucleus (Figs 1b,c, S1). GFP-Xa1<sup>1–1802</sup> was detected in both the nucleus and the cytoplasm, while GFP-Xa1<sup>312–1012</sup> and GFP-Xa1<sup>1008–1802</sup> were localized only in the cytoplasm. Thus, it is likely that the BED domain possesses nuclear-localization activity, which is consistent with a recent report (Zhang *et al.*, 2020).

The *Xoo* strain T7174 (also called MAFF311018) (Ochiai *et al.*, 2005) is incompatible with the rice cultivar Kogyoku, which carries Xa1. *Xoo* T7174 contains 16 TAL effectors including AvrXa7 and Xoo1132 (Ochiai *et al.*, 2005). AvrXa7 and Xoo1132 have 98.9% sequence identity between their N-terminal regions and 98.4% identity between their C-terminal regions, and they have 22.5 and 12.5 repeats in their central repeat regions, respectively (Figs 1d, S2). AvrXa7 and Xoo1132 were each fused to GFP and transiently expressed in rice protoplasts. Fluorescence from both constructs was detected in the nuclei (Figs 1e, S3). The N-terminal region (1–277 amino acids (aa)) and C-terminal region (871–1002 aa) of Xoo1132 were also each fused to GFP. Xoo1132<sup>871–1002</sup>-GFP was localized in the nucleus whereas Xoo1132<sup>1–277</sup>-GFP was detected in both the nucleus and the cytoplasm, as was also observed for the GFP control (Fig. 1e). This result was consistent with the fact that three NLSs exist within the C-terminal region of Xoo1132.

We next performed BiFC experiments to examine the interactions of Xa1 with AvrXa7 and Xoo1132. Full-length Xa1<sup>1–1802</sup> protein was tagged with the C-terminal domain of Venus (Xa1<sup>1–1802</sup>-Vc), while Xoo1132 and AvrXa7 were each tagged with the N-terminal domain of Venus (Xoo1132-Vn and AvrXa7-Vn). Although Xa1<sup>1–1802</sup>-Vc was transfected into rice protoplasts, we failed to detect the corresponding protein (Fig. S4a). Therefore, we tagged each of the Xa1 domains Xa1<sup>1–325</sup>, Xa1<sup>312–1012</sup> and Xa1<sup>1008–1802</sup> with the N-terminal domain of Venus and used them in the BiFC experiments. Fluorescence was detected in the nuclei when Xa1<sup>1–325</sup>-Vc was coexpressed with Xoo1132-Vn or AvrXa7-Vn, but not when AvrXa7-Vn was coexpressed with Xa1<sup>312–1012</sup>-Vc or Xa1<sup>1008–1802</sup>-Vc (Figs 2a, S4a,b). Since protein levels of Xa1<sup>312–1012</sup>-Vc and Xa1<sup>1008–1802</sup>-Vc in the protoplasts were much lower than that of Xa1<sup>1–325</sup>-Vc (Fig. S4a), we could not exclude the possibility that the NB and LRR domains interact with the TAL effectors. However, these data suggest that at least the BED domain of Xa1 associates with these TAL effectors. We also coexpressed Xa1<sup>1–325</sup>-Vc with constructs containing Vn linked to either the N- or C-terminal regions of Xoo1132 (Xoo1132<sup>1–277</sup> or Xoo1132<sup>871–1002</sup>, respectively). The BED (Xa1<sup>1–325</sup>) domain interacted with Xoo1132<sup>871–1002</sup> but not with

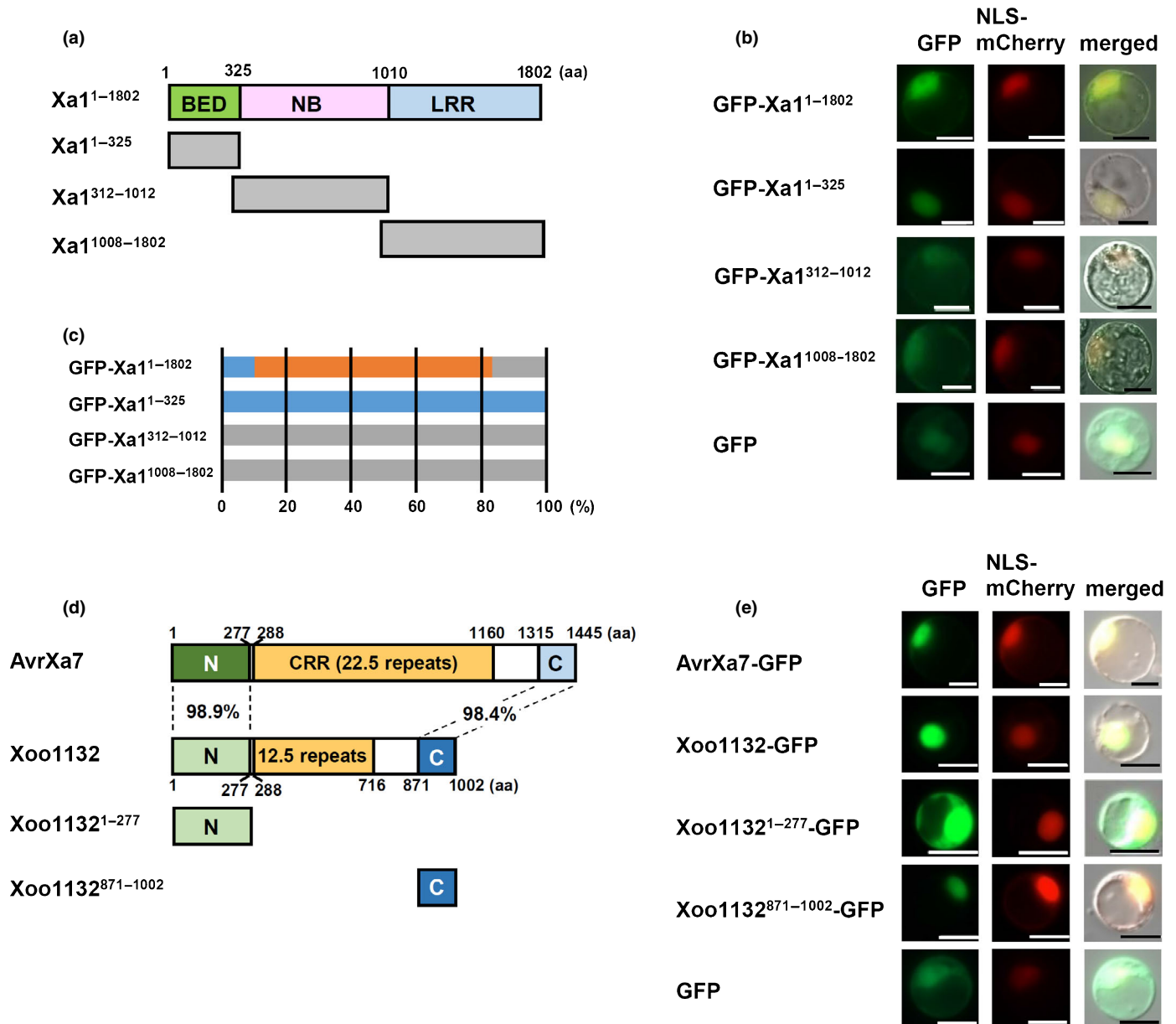


**Fig. 1** Subcellular localization of Xa1, AvrXa7 and Xoo1132. (a) Schematic structures of full-length Xa1<sup>1-1802</sup> and three truncated Xa1 fragments: Xa1<sup>1-325</sup> (1-325 aa), Xa1<sup>312-1012</sup> (312-1012 aa) and Xa1<sup>1008-1802</sup> (1008-1802 aa). Numbers above the boxes indicate amino acid (aa) residues. (b) Subcellular localization of the GFP-fused full-length Xa1 and truncated Xa1 fragments in rice protoplasts. Fluorescence was observed 18 h after transformation. Bar, 10  $\mu$ m. Nuclear localization signal (NLS)-mCherry was used as a nuclear localization marker. (c) Proportions of cells showing nuclear and/or cytoplasmic localization of the Xa1 fragments. Blue and gray boxes indicate nuclear and cytoplasmic localization, respectively. Orange boxes indicate the cells in which fluorescence was detected in both the nuclei and the cytoplasm. (d) Schematic structures of AvrXa7, Xoo1132 and two truncated Xoo1132 fragments. C, C-terminal region; CRR, central repeat region; N, N-terminal region. (e) Subcellular localization of the GFP-fused AvrXa7, Xoo1132 and truncated Xoo1132 fragments in rice protoplasts. Fluorescence was observed 18 h after transformation. Bar, 10  $\mu$ m. NLS-mCherry was used as a nuclear localization marker.

Xoo1132<sup>1-277</sup> in the nucleus (Figs 2a, S4b), even though the GFP constructs indicated that Xoo1132<sup>1-277</sup> and Xoo1132<sup>871-1002</sup> were both localized in the nucleus (Fig. 1e).

To confirm the interaction between the BED domain and the TAL effectors, we carried out a split NanoLuc luciferase complementation assay (Taoka *et al.*, 2021). Xa1<sup>1-325</sup> was fused to the Large BiT of NanoLuc Luciferase (LgBiT, 159 aa), while AvrXa7 and Xoo1132 were each fused to the Small BiT (SmBiT, 12 aa).

The constructs were transfected into rice protoplasts with the *35S-Firefly Luciferase (F-Luc)* construct, and the activities of both luciferases were measured using a microplate luminometer. Consistent with the BiFC experiments, Xa1<sup>1-325</sup> (the BED domain) interacted with both TAL effectors (Figs 2b,c, S5).

The BiFC and split NanoLuc luciferase complementation experiments suggested direct interaction between the BED domain of Xa1 and the TAL effectors. To further test this



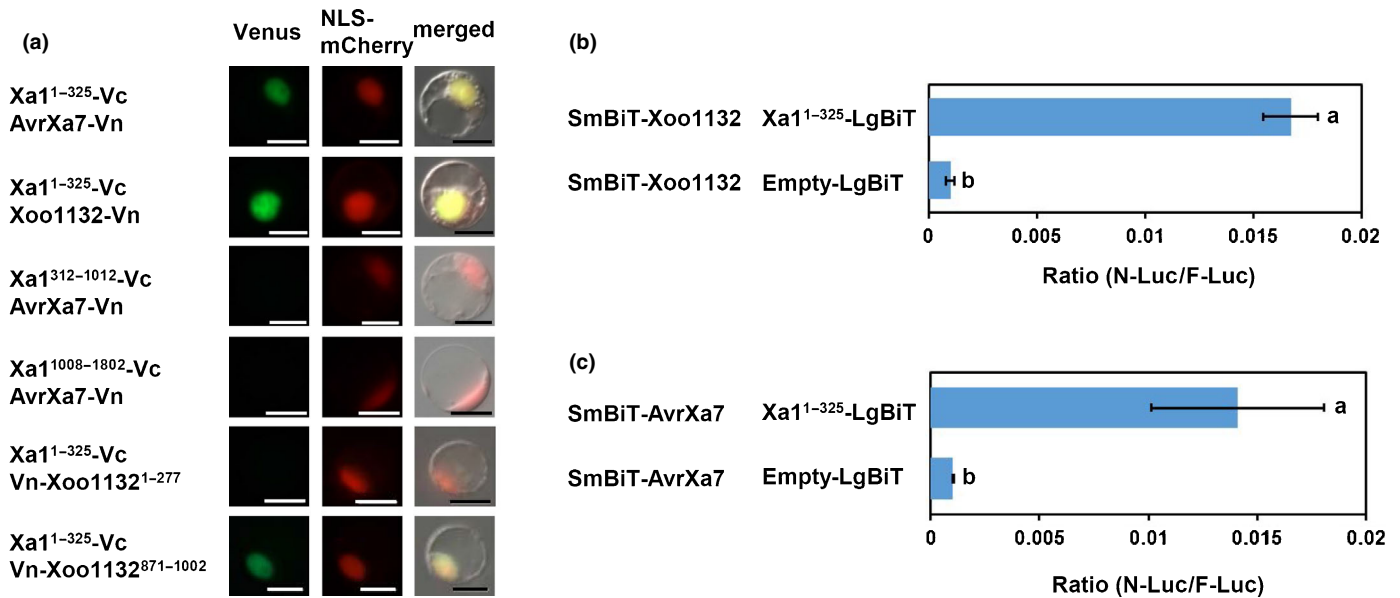


**Fig. 2** Xa1 interacts with AvrXa7 and Xoo1132. (a) Bimolecular fluorescence complementation analysis was used to visualize the interaction between the Xa1 fragments and the TAL effectors in rice protoplasts. Nuclear localization signal (NLS)-mCherry was used as a nuclear localization marker. Bar, 10  $\mu$ m. (b) Quantification of the interaction between the BED domain and Xoo1132. Split NanoLuc luciferase complementation assays were carried out by transient expression of SmBiT-fused Xoo1132 with LgBiT-fused Xa1<sup>1-325</sup>. Values are means  $\pm$  SE. Different letters on the right sides of the data points indicate significant differences (two-sided Welch's *t*-test,  $P < 0.05$ ). (c) Quantification of the interaction between the BED domain and AvrXa7. Split NanoLuc luciferase complementation assays were carried out by transient expression of SmBiT-fused AvrXa7 with LgBiT-fused Xa1<sup>1-325</sup>. Values are means  $\pm$  SE. Different letters on the right sides of the data points indicate significant differences (two-sided Welch's *t*-test,  $P < 0.05$ ).

possibility, we carried out yeast two-hybrid assays. However, interactions were not detected between the BED domain and either of the TAL effectors (Fig. S6). This result suggested that some host factor(s) might be required for the interaction between the BED domain and the TAL effectors.

### OsERF101 interacts with Xa1

To identify host factors involved in the Xa1-mediated immune response, we screened for Xa1 interactors using a yeast two-hybrid assay with the BED domain (Xa1<sup>1-325</sup>) and a rice cDNA library. Initially, we identified 12 candidates (Table S2). Among them, we selected the AP2/ERF-type transcription factor OsERF101/OsRAP2.6 (LOC\_Os04g32620). Our selection was based on the predicted subcellular localization of OsERF101 and the reproducibility of its interaction with the BED domain. In addition, we could not confirm the interaction of the other 11 candidates with the BED domain using any methods other than the yeast two-hybrid assay. Yeast two-hybrid experiments indicated that OsERF101 interacted with the BED domain but not with other Xa1 domains (Figs 3a, S7).

When the OsERF101 protein was fused with GFP (OsERF101-GFP) and transiently expressed in rice protoplasts, the protein was localized to the nucleus (Figs 3b, S8a). We used BiFC assays to demonstrate *in planta* interactions between the BED domain and OsERF101 in the nucleus (Figs 3c, S8b). In addition, we confirmed the interactions between the BED domain and OsERF101 using split NanoLuc luciferase complementation assays (Figs 3d, S8c).

### OsERF101 interacts with the TAL effectors

As described above, we did not detect direct interactions between the BED domain and the TAL effectors in yeast two-hybrid assays. This raised the possibility that OsERF101 may function as a link between Xa1 and the TAL effectors. Therefore, we looked for interactions between OsERF101 and the TAL effectors. In split NanoLuc luciferase complementation assays, OsERF101 showed significant interactions with the TAL effectors (Figs 3e, S8), although the interactions were much weaker than those between the BED domain and the TAL effectors. In addition, the yeast two-hybrid experiments demonstrated direct interactions between OsERF101 and the TAL effectors (Figs 3f, S9). We also used BiFC assays to confirm the interactions between OsERF101 and the TAL effectors (Fig. 3g). However, in these experiments, the BED domain interacted with the TAL effectors even in the absence of OsERF101 (Fig. S10). Furthermore, yeast three-hybrid analysis indicated that the BED domain was not able to interact with the TAL effectors in the presence of OsERF101 (Fig. S11). Thus, although our experiments suggest OsERF101 forms a complex with Xa1 and the TAL effectors, it appears that additional components may be required for the interaction between the BED domain and the TAL effectors.

### OsERF101 positively regulates bacterial blight resistance

We generated an *Xa1* knockout mutant (*xa1*) in the Kogyoku background using the CRISPR/Cas9 system. The mutant carried a two-base deletion located 1022 bp from the start codon

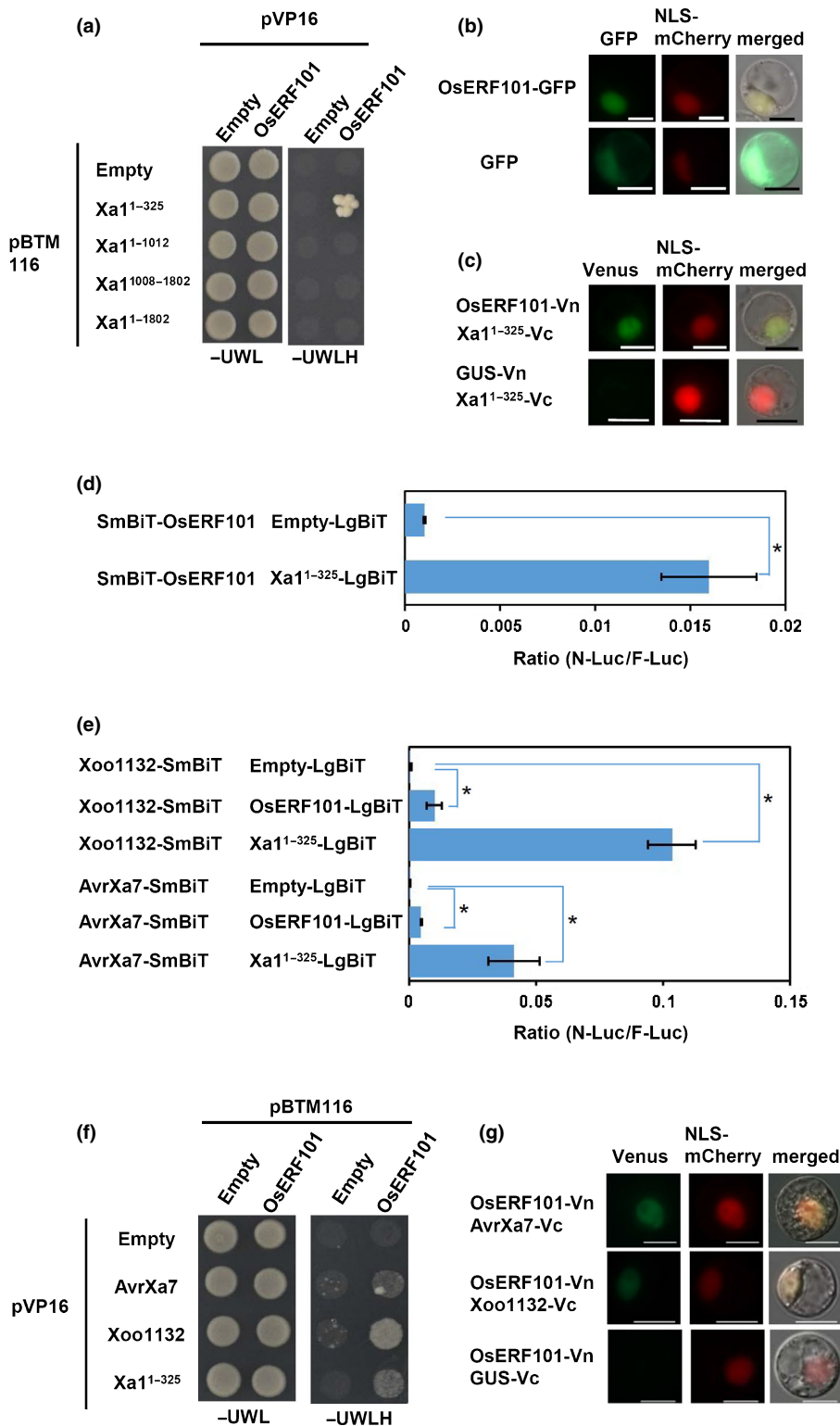


**Fig. 3** OsERF101 interacts with the BED domain of Xa1. (a) Interaction between the Xa1 fragments and OsERF101 in yeast two-hybrid experiments. Growth of yeast colonies on synthetic complete medium without uracil, tryptophan, leucine, and histidine (–UWLH) indicates a positive interaction. (b) Subcellular localization of GFP-fused OsERF101 in rice protoplasts. Fluorescence was observed 18 h after transformation. Bar, 10  $\mu$ m. Nuclear localization signal (NLS)-mCherry was used as a nuclear localization marker. (c) Bimolecular fluorescence complementation analysis was used to visualize the interaction between the BED domain and OsERF101 in rice protoplasts. NLS-mCherry was used as a nuclear localization marker. GUS was used as a negative control. Bar, 10  $\mu$ m. (d) Split NanoLuc luciferase complementation assays for quantification of the interaction between the BED domain and OsERF101. SmBiT-fused OsERF101 and LgBiT-fused Xa1<sup>1-325</sup> were transiently expressed in rice protoplasts, and the luciferase activities were measured. Values are means  $\pm$  SE. An asterisk on the right sides of the data points indicates significant differences (two-sided Welch's *t*-test,  $P < 0.05$ ). (e) Split NanoLuc luciferase complementation assays for quantification of the interaction between OsERF101 and the TAL effectors. SmBiT-fused AvrXa7 or Xoo1132 and LgBiT-fused OsERF101 were transiently expressed in rice protoplasts, and the luciferase activities were measured. Values are means  $\pm$  SE. Asterisks on the right sides of the data points indicate significant differences (two-sided Welch's *t*-test,  $P < 0.05$ ). (f) Interaction between OsERF101 and TAL effectors in yeast two-hybrid experiments. Growth of yeast colonies on –UWLH plates indicates a positive interaction. (g) Bimolecular fluorescence complementation analysis was used to visualize the interaction between OsERF101 and the TAL effectors in rice protoplasts. NLS-mCherry was used as a nuclear localization marker. GUS was used as a negative control. Bar, 10  $\mu$ m.

(Fig. S12a). We then used a needleless syringe-infiltration technique to introduce suspensions of *Xoo* T7174 and *Xoo* T7133 (which is compatible with Kogyoku) into the leaves of wild-type and mutant Kogyoku plants. Wild-type plants developed HR lesions with dark brown edges and weak water soaking when infiltrated with *Xoo* T7174, but showed only water soaking when

infiltrated with *Xoo* T7133 (Fig. 4a). By contrast, the *xa1* mutant did not develop HR lesions when infiltrated with *Xoo* T7174. Consistent with those results, the bacterial population of *Xoo* T7174 was much greater in the *xa1* mutant than in the wild-type plants (Fig. 4b). As mentioned in the Introduction section, AvrXa7 induces *SWEET14* expression by direct binding to its

promoter (Antony *et al.*, 2010). We observed stronger induction of *SWEET14* expression in the *xa1* mutant than in the wild-type plants after infiltration with *Xoo* T7174 (Fig. 4c).

To elucidate the function of OsERF101 in bacterial blight resistance, we transformed wild-type Kogyoku plants with an overexpression construct of *OsERF101* driven by the CaMV 35S promoter (Fig. S13). When these plants were infiltrated with the *Xoo* T7174 suspension, they exhibited a stronger HR than the wild-type plants, as indicated by the development of HR lesions without water soaking (Fig. 4a). Consistent with the stronger HR, both bacterial growth and *SWEET14* expression were reduced in the infiltrated *OsERF101-OX* plants when compared with nontransformed plants (Fig. 4b,c). These results indicate that OsERF101 plays a positive role in resistance to bacterial blight.

### Knockout of *OsERF101* results in enhanced resistance

To analyze the involvement of OsERF101 in Xa1-mediated immunity, we used the CRISPR/Cas9 system to generate two knockout mutant lines of *OsERF101* in the Kogyoku background. Both *oserf101-1* and *oserf101-2* carried frame-shift mutations located *c.* 220 bp from the start codon (Fig. S12b). When either of these lines was infiltrated with *Xoo* T7174, it exhibited light brown lesions that had a different appearance from the typical Xa1-induced HR lesion (Fig. 4a). This result was unexpected because OsERF101 was predicted to function as a positive regulator of rice immunity. However, bacterial growth and *SWEET14* expression were strongly suppressed in the *oserf101* mutants after infiltration with *Xoo* T7174 (Fig. 4b,c), as we also observed in the *OsERF101-OX* plants. Thus, both the overexpression of *OsERF101* and the knockout of *OsERF101* induced strong resistance to rice bacterial blight.

### The enhanced resistance of *OsERF101-OX* and *oserf101* plants depends upon Xa1

The *Xoo* strain T7133 is compatible with Kogyoku (Ogawa *et al.*, 1978) and produces disease lesions with water soaking when infiltrated into the leaves of Kogyoku (Fig. 4a). We determined the genome sequence of *Xoo* T7133 and found that it contains a type-A iTAL effector gene (Yoshihisa *et al.*, 2021). Thus far, all *Xoo* strains containing type-A iTAL effectors have been observed to inhibit Xa1-mediated immunity in rice (Ji *et al.*, 2020). Therefore, we expect that the iTAL effector of *Xoo* T7133 would also inhibit Xa1-mediated resistance.

We infiltrated a suspension of *Xoo* T7133 into the leaves of the *OsERF101-OX* plants. The *OsERF101-OX* leaves did not exhibit HR lesions as they did with *Xoo* T7174, but instead displayed water-soaked disease lesions (Fig. 4a). Consistent with this result, the bacterial populations of *Xoo* T7133 were increased in the *OsERF101-OX* plants, as they were in the wild-type plants and the *xa1* mutant (Fig. 4d). In addition, expression levels of *SWEET14* in the *Xoo* T7133-infiltrated *OsERF101-OX* plants were similar to those in the wild type and the *xa1* mutant (Fig. 4e). We also infiltrated a suspension of *Xoo* T7133 into the

leaves of the *oserf101* knockout mutant lines. The atypical HR lesions induced by infection with *Xoo* T7174 were not observed after infection with *Xoo* T7133 (Fig. 4a). As observed in the *OsERF101-OX* plants, the infiltrated *oserf101* leaves developed water-soaked disease lesions (Fig. 4a), along with wild-type levels of bacterial growth and *SWEET14* expression (Fig. 4d,e). Because the iTAL effector of *Xoo* T7133 probably suppresses the immune responses induced via the recognition of TAL effectors by Xa1, these results suggest that the enhanced resistance of the *OsERF101-OX* and *oserf101* plants may be Xa1-dependent.

To confirm that the enhanced resistance induced by both the overexpression and knockout of *OsERF101* in the Kogyoku background is dependent on Xa1, we next conducted transient assays to analyze Xa1-mediated cell death. Kogyoku protoplasts were transfected with a dexamethasone (DEX)-inducible *AvrXa7* construct (*pTA7002::AvrXa7*) along with a p35S-NanoLuc luciferase construct, and cell death levels were estimated by measuring the luciferase activity after mock or DEX treatments. DEX treatment induced cell death in the wild-type Kogyoku protoplasts (Fig. S14a). The *AvrXa7*-induced cell death in Kogyoku protoplasts was reduced by silencing of *Xa1*. Silencing of *Xa1* also suppressed cell death in the *OsERF101-OX* and *oserf101* protoplasts (Fig. S14b,c). These results indicate that the hypersensitive response induced in the *OsERF101-OX* and *oserf101* cells is mainly dependent on Xa1, although weak contributions of other factors in addition to Xa1 cannot be excluded.

To further confirm that the enhanced resistance induced by the overexpression and knockout of *OsERF101* is dependent on Xa1, we generated transgenic plants overexpressing *OsERF101* and created knockout mutants of *OsERF101* in the rice cultivar Nipponbare background (Fig. S12c). Nipponbare does not possess the *Xa1* gene. Similar to wild-type Nipponbare leaves, *OsERF101-OX* and *oserf101* Nipponbare leaves developed water-soaked disease lesions when infiltrated with *Xoo* T7174 (Fig. 5a). In addition, we analyzed bacterial growth and expression of *SWEET14* in the Nipponbare lines after infiltration with *Xoo* T7174 (Fig. 5b,c). The results indicated that neither the overexpression nor the knockout of *OsERF101* caused enhanced resistance to *Xoo* T7174 in the Nipponbare background. Thus, it is likely that the enhanced resistance induced by both the overexpression and knockout of *OsERF101* in the Kogyoku background is dependent on Xa1.

As describe above, neither the overexpression nor the knockout of *OsERF101* in the Kogyoku background altered its response to the compatible pathogen *Xoo* T7133. Previously, OsERF101/OsRAP2.6 was reported to positively regulate resistance to a compatible blast fungus. Therefore, we analyzed blast resistance using the *OsERF101-OX* and *oserf101* plants in the Nipponbare background. Unlike the previous report, the *OsERF101-OX* plants exhibited enhanced susceptibility to a compatible isolate (Ao92-06-2) of blast fungus (Fig. S15), whereas the *oserf101* mutation did not affect the resistance. This inconsistency with the previous report might be due to the differences in rice varieties and the fungal isolates. Thus, it seems that OsERF101 may be involved in the general immune responses against compatible isolates of blast fungus. On the other hand, it is likely that

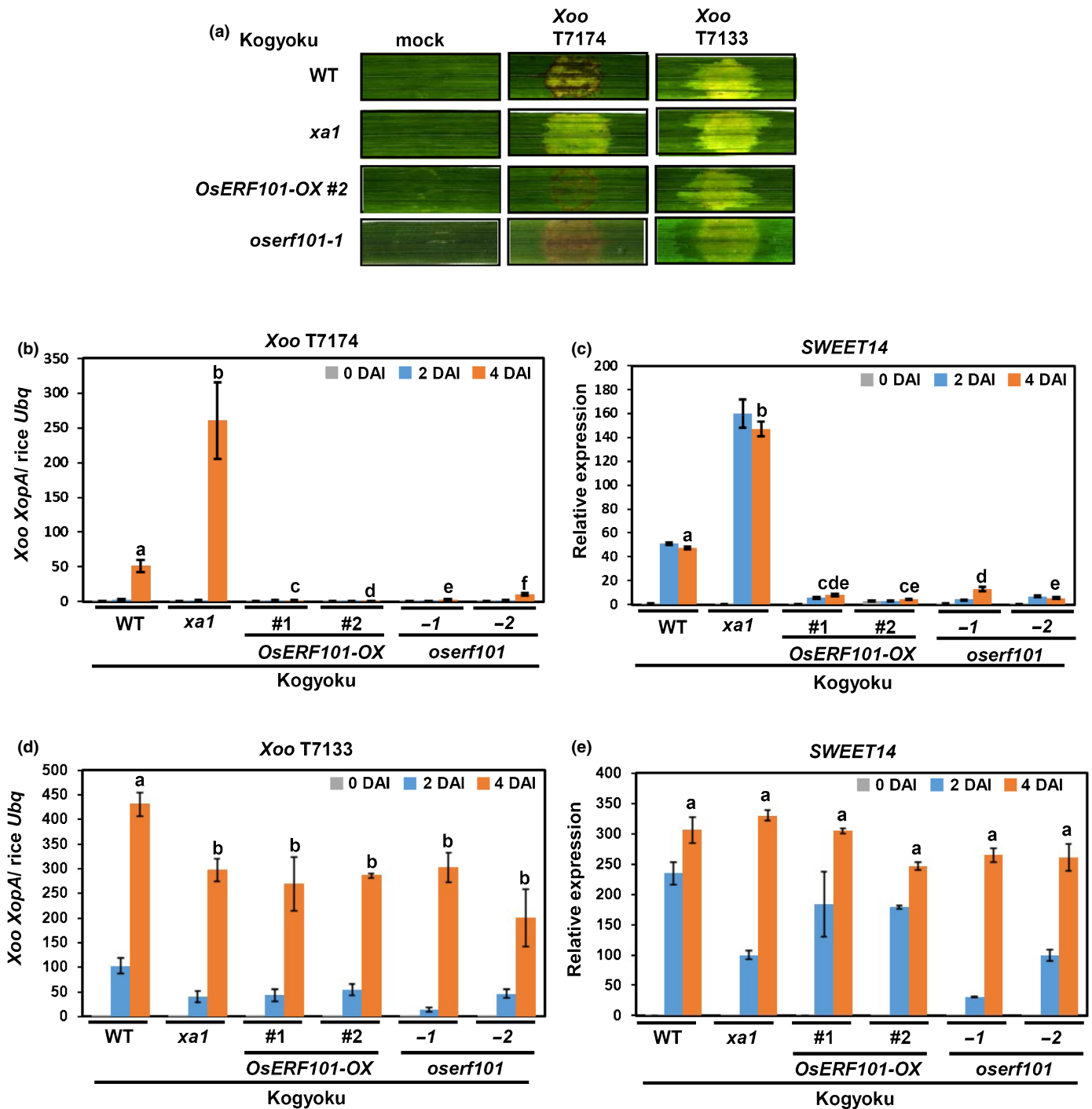


**Fig. 4** *OsERF101-OX* and *oserf101* enhance bacterial blight resistance in the cv Kogyoku background. (a) Hypersensitive responses of wild-type (WT), the *OsERF101-OX* and *oserf101* plants in the Kogyoku background. Suspensions of *Xanthomonas oryzae* pv *oryzae* (Xoo) T7174 or Xoo T7133 were injected into the leaves of 3-wk-old seedlings. Photos were taken at 4 d after inoculation (DAI). (b) The bacterial populations of Xoo T7174 in the *OsERF101-OX* and *oserf101* plants were analyzed by quantitative real-time PCR. The data indicate DNA levels of the *X. oryzae* *XopA* gene relative to those of the rice *ubiquitin* gene. Values are means  $\pm$  SE. Different letters above the 4 DAI data points indicate significant differences (two-sided Welch's *t*-test,  $P < 0.01$ ). (c) Expression of *SWEET14* in the *OsERF101-OX* and *oserf101* plants after infection with Xoo T7174. Transcript levels were measured by quantitative real-time PCR. Values are means  $\pm$  SE. Different letters above the 4 DAI data points indicate significant differences (two-sided Welch's *t*-test,  $P < 0.01$ ). (d) The bacterial populations of Xoo T7133 in the *OsERF101-OX* and *oserf101* plants in the Kogyoku background were analyzed by quantitative real-time PCR. The data indicate DNA levels of the *X. oryzae* *XopA* gene relative to those of the rice *ubiquitin* gene. Values are means  $\pm$  SE. Different letters above the 4 DAI data points indicate significant differences (two-sided Welch's *t*-test,  $P < 0.05$ ). (e) Expression of *SWEET14* in the *OsERF101-OX* and *oserf101* plants after infection with Xoo T7133. Transcript levels were measured by quantitative real-time PCR. Values are means  $\pm$  SE. Different letters above the 4 DAI data points indicate significant differences (two-sided Student's *t*-test,  $P < 0.05$ ).



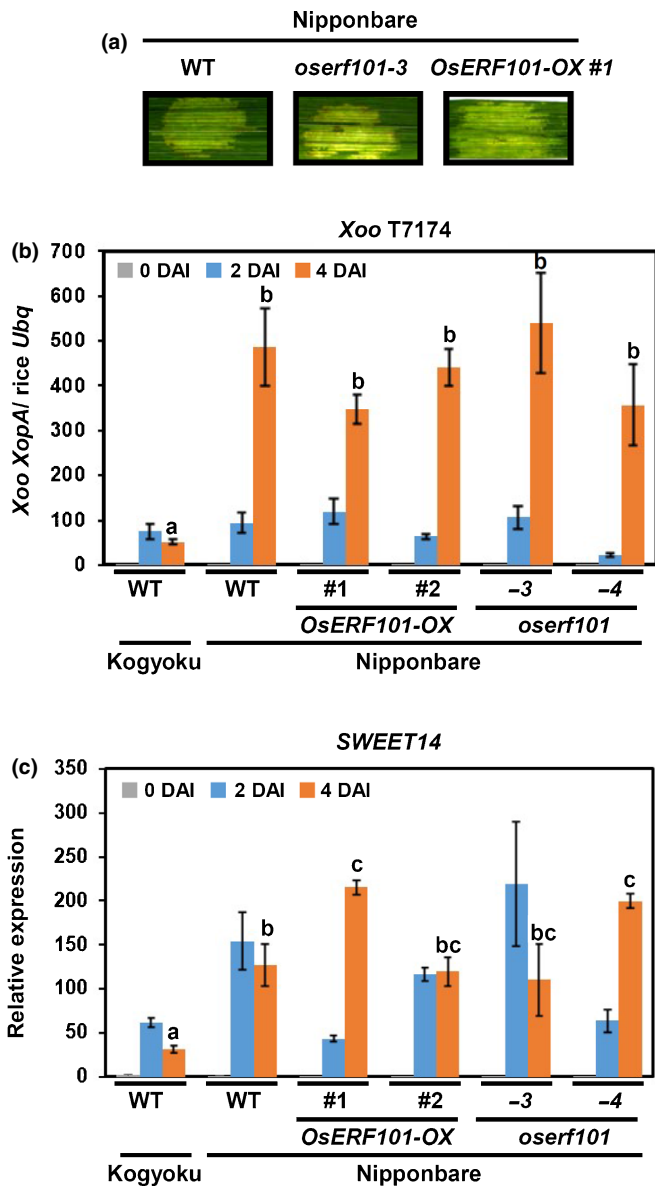


**Fig. 5** Enhanced resistance of the *OsERF101-OX* and *oserf101* plants depends on Xa1. (a) Disease symptoms of wild-type (WT), *OsERF101-OX* and *oserf101* plants in the cv Nipponbare background. A suspension of *Xanthomonas oryzae* pv *oryzae* (*Xoo*) T7174 was injected into the leaves of 3-wk-old seedlings. Photos were taken at 4 d after inoculation (DAI). (b) The bacterial populations of *Xoo* T7174 in the *OsERF101-OX* and *oserf101* plants in the Nipponbare background were analyzed by quantitative real-time PCR. Data indicate DNA levels of the *X. oryzae* *XopA* gene relative to those of the rice *ubiquitin* gene. Values are means  $\pm$  SE. Different letters above the 4 DAI data points indicate significant differences (two-sided Welch's *t*-test,  $P < 0.01$ ). (c) Expression of *SWEET14* in the *OsERF101-OX* and *oserf101* plants in the Nipponbare background after infection with *Xoo* T7174. Transcript levels were measured by quantitative real-time PCR. Values are means  $\pm$  SE. Different letters above the 4 DAI data points indicate significant differences (two-sided Student's *t*-test,  $P < 0.01$ ).

*OsERF101* contributes specifically to Xa1-mediated immunity in bacterial blight resistance.

To test whether *OsERF101* is involved in other incompatible interactions between rice and *Xoo*, we analyzed cell death responses

induced by the bacterial blight resistance gene *Xa10*. It has been reported that *Xa10* expression is directly activated by the TAL effector AvrXa10, which confers race-specific resistance to rice bacterial blight (Tian *et al.*, 2014). Transient expression of *Xa10* induced similar levels of cell death in wild-type, *OsERF101-OX* and *oserf101* rice protoplasts (Fig. S16). These results suggest that *OsERF101* does not contribute to Xa10-induced immunity.

### Overexpression and knockout of *OsERF101* induce different types of immune responses

We observed that the *OsERF101-OX* lines and *oserf101* knockout lines in the Kogyoku background displayed different types of HR lesions after infiltration with *Xoo* T7174 (Fig. 4a). This suggested that *OsERF101-OX* and *oserf101* may have different effects on the expression of downstream genes. Therefore, we carried out RNA-seq analyses using mRNAs purified from wild-type, *OsERF101-OX* and *oserf101* leaves at 2 d after mock treatment or infiltration with *Xoo* T7174. We identified 5390 DEGs ( $q$ -value  $< 0.01$ , fold-change  $> 4$ ) whose expression levels were up- or downregulated when compared with their expression after mock treatment (Fig. 6a; Table S3). There were larger numbers of DEGs in wild-type leaves than in *OsERF101-OX* or *oserf101* leaves. Because bacterial growth in the *OsERF101-OX* and *oserf101* leaves was much lower than that in wild-type leaves (Fig. 4b,c), it seems that the immune responses may be induced at earlier time points in the overexpression and knockout lines. Venn diagrams also indicated that the overexpression of *OsERF101* affects the expression of a largely different set of downstream genes than those affected by the knockout mutation of *OsERF101* (Fig. 6a). In addition, we carried out GO enrichment analysis of the DEGs shown in Table S3. The results indicate that many DEGs are involved in regulation of response to stimulus (Table S4).

We performed clustering analysis using the 1630 DEGs with transcripts per million (TPM)  $> 50$  (Fig. 6b; Table S4). The experiments revealed four clusters specific to either *oserf101* or *OsERF101-OX*. Clusters #1 and #2 were downregulated specifically in *oserf101* and *OsERF101-OX*, respectively. Clusters #3 and #4 were upregulated specifically in *OsERF101-OX* and *oserf101*, respectively. These clusters contained many genes that are predicted to be involved in immune responses (Table S5). Thus, it is likely that the mechanism by which the knockout of *OsERF101* enhances Xa1-mediated immunity is different from the mechanism by which *OsERF101* overexpression enhances immunity. Our results suggest two regulatory pathways, both mediated by Xa1. In one pathway, *OsERF101* functions as a positive immune regulator, whereas the other pathway is negatively regulated by *OsERF101*.

To further investigate the different transcriptional regulation pathways between the *OsERF101-OX* and *oserf101* plants, we carried out enrichment analyses of *cis* regulatory elements in the promoter sequences of the DEGs discussed above. We found that the E-box 'CANNTG', the *cis*-element recognized by basic-Helix-Loop-Helix (bHLH)-type transcription factors, is enriched in the 360 DEGs specifically downregulated in the *OsERF101-*

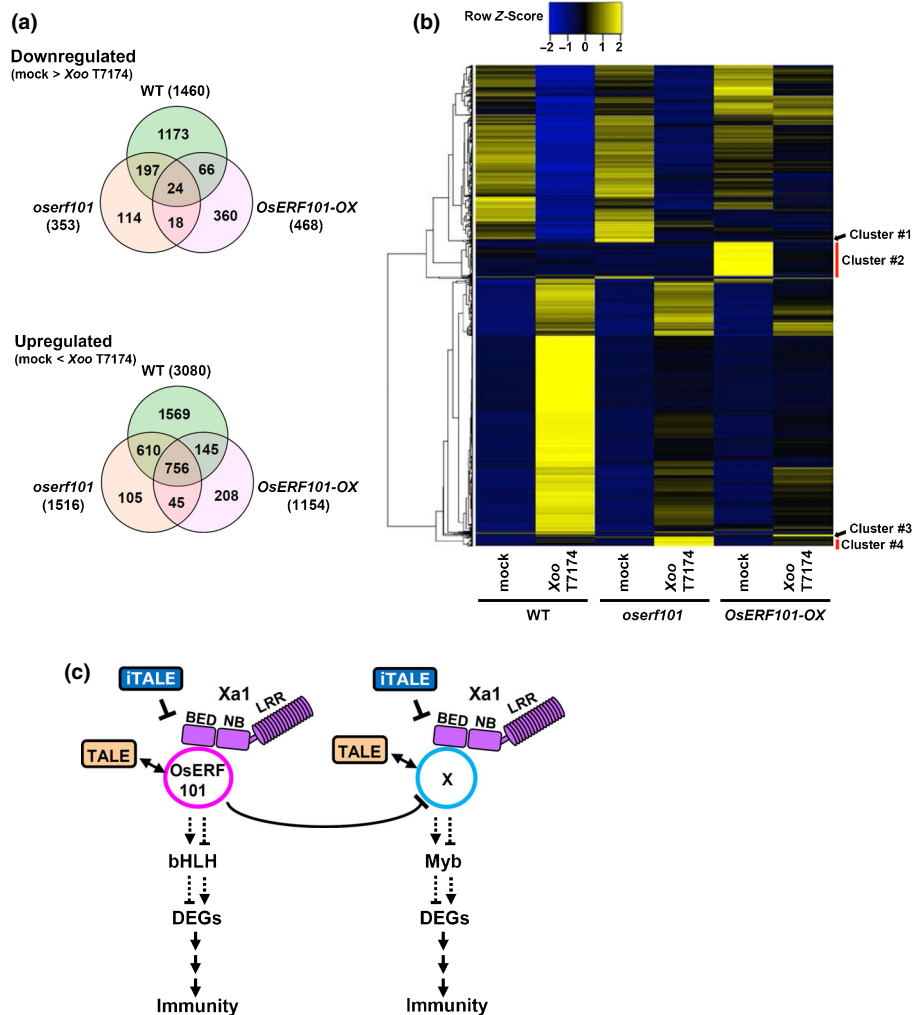


**Fig. 6** *OsERF101-OX* and *oserf101* plants activate different Xa1-mediated immunity pathways. (a) Comparative analysis of transcriptomes in wild-type (WT), *OsERF101-OX* and *oserf101* plants in the cv Kogyoku background. RNA-seq analysis was carried out using leaves at 2 d after infiltration with *Xanthomonas oryzae* pv *oryzae* (Xoo) T7174 or mock treatment. Venn diagrams show the numbers of specifically regulated differentially expressed genes (DEGs), and DEGs overlapping among wild-type, *OsERF101-OX* and *oserf101* plants. (b) The 1630 DEGs with transcripts per million (TPM) > 50 in any treatment were used in clustering analyses. The results revealed four clusters that are specifically up- or downregulated in *oserf101* or *OsERF101-OX* plants. (c) Proposed model for *OsERF101*-mediated immunity. In this model, *OsERF101* interacts with Xa1 and a TAL effector (TALE), and positively regulates Xa1-mediated immunity via a pathway regulated by bHLH transcription factor(s). *OsERF101* may negatively regulate a putative Factor X, which functions as a positive regulator of Xa1-mediated immunity via a pathway regulated by Myb transcription factor(s). In this model, the bHLH or Myb transcription factors, which are positively regulated by *OsERF101* or the X factor, respectively, may suppress expression of DEGs. On the other hand, the bHLH or Myb transcription factors, which are negatively regulated by *OsERF101* or the X factor, respectively, may activate expression of DEGs. Depletion of *OsERF101* may lead to enhanced Factor X-mediated immunity. iTALE effectors (iTALE) inhibit Xa1 function and block these immunity pathways. The blunt-ended arrow indicates inhibition. The dashed arrows indicate that the connections were not experimentally confirmed.

*OX* plants (Figs 6a, S17), whereas no enrichment was observed in the 208 DEGs specifically upregulated in the *OsERF101-OX* plants. On the other hand, the *cis*-element for Myb-type transcription factors is enriched in the 114 DEGs specifically downregulated in the *oserf101* plants (Figs 6a, S18). As in the *OsERF101-OX* plants, no enrichment was detected in the 105 DEGs specifically upregulated in the *oserf101* plant. Thus, it is likely that overexpression of *OsERF101* enhances resistance through bHLH-type transcription factors, while the knockout of *OsERF101* enhances resistance through Myb-type transcription factors.

## Discussion

Plants contain large numbers of NLR proteins. Some NLRs possess integrated decoy domains that are targeted by pathogen effectors. These integrated decoy domains mimic other effector targets whose binding to the effectors leads to disease development. Although BED was predicted to be an integrated decoy domain (Zuluaga *et al.*, 2017), direct evidence for this has not yet been obtained. Here, we showed that Xa1 forms complexes with the Xoo TAL effectors AvrXa7 and Xoo1132 via the BED domain, although direct interaction between the BED domain

and the TAL effectors was not detected. We also found that the BED domain and the TAL effectors interact with the transcription factor OsERF101. Overexpression of *OsERF101* enhanced Xa1-mediated disease resistance, suggesting that OsERF101 plays a pivotal role in Xa1-mediated recognition of the TAL effectors and immune activation. Taken together, our results suggested that OsERF101 is a positive regulator in Xa1-mediated immunity.

On the other hand, we found that the *oserrf101* knockout mutants also showed enhanced resistance to *Xoo* T7174. Interestingly, the HR lesions of the Kogyoku *oserrf101* knockout mutants exhibited quite different characteristics from those of wild-type and *OsERF101-OX* plants. Furthermore, the *OsERF101-OX* plants and the *oserrf101* mutants influenced the transcription of largely different sets of downstream genes. Enrichment analyses of *cis* regulatory elements suggested that these different sets of downstream genes are regulated by different types of transcription factors: bHLH-type transcription factors in *OsERF101-OX* plants and Myb-type transcription factors in *oserrf101* plants. This phenomenon suggests an additional Xa1-mediated immune pathway that is negatively regulated by OsERF101. Based on these data, we propose a model for Xa1-OsERF101-mediated immune signaling by hypothesizing the existence of an 'X factor' involved in Xa1-mediated immunity (Fig. 6c). In this model, both OsERF101 and the X factor positively regulate Xa1-mediated immunity, but OsERF101 has the ability to inhibit activity of the X factor. Overexpression of *OsERF101* induces an immunity pathway mediated by bHLH transcription factors, but may suppress the X factor. Knockout of *OsERF101* results in enhancement of the X factor-mediated immune response through Myb transcription factors. This model is consistent with two observations: the enhanced resistance to *Xoo* T7174, induced by either the overexpression of *OsERF101* or the knockout of *OsERF101* in the Kogyoku background, is not observed with *Xoo* T7133, which carries an iTAL effector; and neither *OsERF101-OX* nor the *oserrf101* mutation enhances *Xoo* T7174 resistance in the Nipponbare background, which does not carry Xa1. Note here that *Xoo* T7174 also contains an iTAL effector named Tal3b, but Tal3b is not functional in *Xoo* T7174 for unknown reasons (Ji *et al.*, 2016).

Rice contains 163 AP2/ERF-type transcription factors (Sharoni *et al.*, 2011). The AP2/ERF transcription factors positively or negatively regulate abiotic and biotic stress and hormone responses (Xie *et al.*, 2019). In fact, OsERF101/OsRAP2.6 has been reported to participate in resistance to rice blast (Wamaitha *et al.*, 2012), leaf senescence (Lim *et al.*, 2020) and drought stress (Jin *et al.*, 2018). Recently, OsERF101 was reported to regulate the transcription of *OsMYC2*, which encodes a bHLH transcription factor, by directly binding its promoter (Lim *et al.*, 2020). In addition, overexpression of *OsMYC2* is known to enhance resistance to bacterial blight (Uji *et al.*, 2016). These observations suggest that the OsERF101–OsMYC2 module may control *Xoo* resistance. In this study, we found that the *cis*-elements of the bHLH transcription factors are enriched in the DEGs downregulated in the *OsERF101-OX* plants. Therefore, the bHLH transcription factors including OsMYC2, which are positively

regulated by OsERF101, may suppress expression of the corresponding DEGs, although it is possible that OsERF101 may inhibit the bHLH transcription factors that positively regulate expression of the DEGs (Fig. 6c). In a similar way, it appears that the Myb transcription factors may function downstream of the X factor. Further analysis will be required to elucidate how bHLH and Myb transcription factors regulate the Xa1-mediated immunity.

The *Xa1* alleles *Xa2*, *Xa14*, *Xa45* and *Xo1* also encode BED-NLR proteins. The BED and NB domains are highly homologous among these Xa1 allelic members. However, they are differentiated by the numbers of repeats in their C-terminal LRR regions (Ji *et al.*, 2020; Read *et al.*, 2020; Zhang *et al.*, 2020), and they confer different resistance spectra to races of *Xoo*. The differences in the LRR regions suggest that the LRR domains may be the determinants of race specificity to *Xoo*. Since the immune responses mediated by these allelic members are suppressed by iTAL effectors (Ji *et al.*, 2020), it is likely that they all recognize the TAL effectors. However, here we did not detect interactions between the LRR domain of Xa1 and the two TAL effectors. Instead, our BiFC and split NanoLuc luciferase complementation assays suggested the formation of a complex involving a TAL effector, OsERF101, and the BED domain of Xa1. Therefore, it is possible that the differences among the LRR regions of the Xa1 allelic members may affect either the formation of the tertiary complex or the LRR domain-mediated recognition of the tertiary complex.

The yeast two-hybrid experiments indicated that OsERF101 directly interacts with Xa1 and the TAL effectors. In addition, OsERF101 regulates Xa1-dependent immunity, and we speculate that the putative X factor also regulates Xa1-dependent immunity. Host factors that are targeted by pathogen effectors and act as coreceptors with NLRs are referred to as sensing decoys (Paulus & van der Hoorn, 2018). Therefore, it is possible that OsERF101 and the X factor may be sensing decoys targeted by the TAL effectors, and that they function as coreceptors with Xa1. Since sensing decoys generally promote effector recognition in the presence of their cognate NLR proteins (Paulus & van der Hoorn, 2018), this scenario is consistent with the fact that the overexpression and knockout mutation of *OsERF101* enhanced Xa1-dependent immunity in the Kogyoku background, but not in the Nipponbare background. However, since our data suggest that OsERF101 activates immunity through bHLH transcription factors, it appears that OsERF101 also contributes to the activation of Xa1-mediated immune signaling.

Consistent with recent reports (Read *et al.*, 2020; Xu *et al.*, 2021), we found that Xa1 is localized in the nucleus. Our data indicated that the BED domain can confer nuclear localization. Thus, it is likely that Xa1 recognizes the TAL effectors in the nucleus. In fact, the inhibition of Xa1-mediated immunity by the iTAL effectors requires the nuclear localization of the iTAL effectors (Ji *et al.*, 2016). These data suggest strongly that Xa1 activates immune responses within the nucleus. Recent investigations using coimmunoprecipitation indicated that the Xa1 allelic member Xo1 interacts with the iTAL effector Tal2h (Read *et al.*, 2020), although it is not yet known whether the interaction



is direct or indirect. Although the molecular mechanisms of how the iTAL effectors inhibit Xa1-mediated immunity are not yet understood, it is possible that the iTAL effectors may suppress Xa1 through OsERF101 or the putative X factor.

It has been reported that the BED domains form dimers (Zhang *et al.*, 2020). This suggests that oligomerization to form resistosomes may occur in BED NLRs, as is the case with other NLR proteins (Wang *et al.*, 2019; Ma *et al.*, 2020; Martin *et al.*, 2020). If interactions among the BED domain, OsERF101 and the TAL effectors alter the tertiary structure of the Xa1 protein, it is possible that this structural change may facilitate oligomerization through the BED domains. Recent structural studies of resistosomes using cryoelectron microscopy are beginning to reveal how NLRs activate immunity (Wang *et al.*, 2019; Ma *et al.*, 2020; Martin *et al.*, 2020). Some NLRs with the N-terminal Toll-interleukin-1 receptor domain induce cell death through their nicotinamide adenine dinucleotide hydrolase activity and/or their cyclic nucleotide monophosphate synthetase activity (Horsefield *et al.*, 2019; Wan *et al.*, 2019; Yu *et al.*, 2022). On the other hand, several NLRs with N-terminal coiled coil domains function as plasma membrane-localized calcium-permeable channels (Bi *et al.*, 2021; Jacob *et al.*, 2021). However, the molecular mechanisms by which nuclear-localized NLRs activate immunity in plants are still unknown. The present report on the interaction between Xa1 and OsERF101 in initiation of the immune response provides new insights into NLR-mediated immunity.


## Acknowledgements

We thank Dr. Seiji Tsuge and Dr. Bing Yang for valuable suggestions concerning TAL effectors, Masaki Endo for the CRISPR/Cas9 expression constructs, Ken-ichiro Taoka for the split Nano-Luc Luciferase assay constructs, Tetsuya Nakazaki and Kazusa Nishimura for use of their glasshouse, and Nao Hayata, Maho Izumitani, Shunsuke Ando and Toshikazu Ohuchi for technical assistance. We also thank the Ministry of Agriculture Fisheries and Forestry of Japan (MAFF) for providing *Magnaporthe oryzae* isolates, Ao92-06-2. This research was supported by Grants-in-Aid for Scientific Research (A) (19H00945), for Scientific Research on Innovative Areas (18H04789), for Exploratory Research (20K21320), Strategic International Collaborative Research project promoted by the Ministry of Agriculture, Forestry and Fisheries, Tokyo, Japan (JPJ0088379) and Basic Science Research Projects from the Mitsubishi Foundation to TK; by Grants-in-Aid for Scientific Research (JP19K06061) and Basic Science Research Projects from the Sumitomo Foundation to KY.


## Author contributions


AY, SY and TK designed the research. AY, SY, SS, SM and KY performed the experiment. MS and AM analyzed RNA-seq data. AY, SY and TK wrote the manuscript. AY and SY contributed equally to this work as first coauthors.

## ORCID

Tsutomu Kawasaki  <https://orcid.org/0000-0003-2579-2000>

Akira Mine  <https://orcid.org/0000-0002-4822-4009>

Motoki Shimizu  <https://orcid.org/0000-0002-5622-5554>

Koji Yamaguchi  <https://orcid.org/0000-0002-3167-7079>

## Data availability

The data that support the findings of this study are available from the corresponding author upon reasonable request.

## References

- Antony G, Zhou J, Huang S, Li T, Liu B, White F, Yang B. 2010. Rice *xa13* recessive resistance to bacterial blight is defeated by induction of the disease susceptibility gene *Os-11N3*. *Plant Cell* 22: 3864–3876.
- Bi G, Su M, Li N, Liang Y, Dang S, Xu J, Hu M, Wang J, Zou M, Deng Y *et al.* 2021. The ZAR1 resistosome is a calcium-permeable channel triggering plant immune signaling. *Cell* 184: 3528–3541.
- Boch J, Scholze H, Schornack S, Landgraf A, Hahn S, Kay S, Lahaye T, Nickstadt A, Bonas U. 2009. Breaking the code of DNA binding specificity of TAL-type III effectors. *Science* 326: 1509–1512.
- Chen L, Hamada S, Fujiwara M, Zhu T, Thao NP, Wong HL, Krishna P, Ueda T, Kaku H, Shibuya N *et al.* 2010. The Hop/Sti1-Hsp90 chaperone complex facilitates the maturation and transport of a PAMP receptor in rice innate immunity. *Cell Host & Microbe* 7: 185–196.
- Dangl JL, Horvath DM, Staskawicz BJ. 2013. Pivoting the plant immune system from dissection to deployment. *Science* 341: 746–751.
- Dou D, Zhou JM. 2012. Phytopathogen effectors subverting host immunity: different foes, similar battleground. *Cell Host & Microbe* 12: 484–495.
- Hiei Y, Ohta S, Komari T, Kumashiro T. 1994. Efficient transformation of rice (*Oryza sativa* L.) mediated by *Agrobacterium* and sequence analysis of the boundaries of the T-DNA. *The Plant Journal* 6: 271–282.
- van der Hoorn RA, Kamoun S. 2008. From guard to decoy: a new model for perception of plant pathogen effectors. *Plant Cell* 20: 2009–2017.
- Horsefield S, Burdett H, Zhang X, Manik MK, Shi Y, Chen J, Qi T, Gilley J, Lai JS, Rank MX *et al.* 2019. NAD<sup>+</sup> cleavage activity by animal and plant TIR domains in cell death pathways. *Science* 365: 793–799.
- Ishikawa K, Yamaguchi K, Sakamoto K, Yoshimura S, Inoue K, Tsuge S, Kojima C, Kawasaki T. 2014. Bacterial effector modulation of host E3 ligase activity suppresses PAMP-triggered immunity in rice. *Nature Communications* 5: 5430.
- Jacob P, Kim NH, Wu F, El-Kasbi F, Chi Y, Walton WG, Furzer OJ, Lietzan AD, Sunil S, Kempthorn K *et al.* 2021. Plant “helper” immune receptors are Ca<sup>2+</sup>-permeable nonselective cation channels. *Science* 373: 420–425.
- Ji C, Ji Z, Liu B, Cheng H, Liu B, Liu S, Yang B, Chen G. 2020. *Xa1* allelic R genes activate rice blight resistance suppressed by interfering TAL effectors. *Plant Communications* 1: 100087.
- Ji Z, Ji C, Liu B, Zou L, Chen G, Yang B. 2016. Interfering TAL effectors of *Xanthomonas oryzae* neutralize R-gene-mediated plant disease resistance. *Nature Communications* 7: 13435.
- Jin Y, Pan W, Zheng X, Cheng X, Liu M, Ma H, Ge X. 2018. OsERF101, an ERF family transcription factor, regulates drought stress response in reproductive tissues. *Plant Molecular Biology* 98: 51–65.
- Jones JD, Vance RE, Dangl JL. 2016. Intracellular innate immune surveillance devices in plants and animals. *Science* 354: aaf6395.
- Kim D, Langmead B, Salzberg SL. 2015. HISAT: a fast spliced aligner with low memory requirements. *Nature Methods* 12: 357–360.
- Liao Y, Smyth GK, Shi W. 2014. FEATURECOUNTS: an efficient general purpose program for assigning sequence reads to genomic features. *Bioinformatics* 30: 923–930.
- Lim C, Kang K, Shim Y, Sakuraba Y, An G, Paek NC. 2020. Rice ETHYLENE RESPONSE FACTOR 101 promotes leaf senescence through Jasmonic acid-



- mediated regulation of OsNAP and OsMYC2. *Frontiers in Plant Science* 11: 1096.
- Lo CC, Chain PS. 2014. Rapid evaluation and quality control of next generation sequencing data with FAQCs. *BMC Bioinformatics* 15: 366.
- Ma S, Lapin D, Liu L, Sun Y, Song W, Zhang X, Logemann E, Yu D, Wang J, Jirschtzka J *et al.* 2020. Direct pathogen-induced assembly of an NLR immune receptor complex to form a holoenzyme. *Science* 370: eable3069.
- Martin R, Qi T, Zhang H, Liu F, King M, Toth C, Nogales E, Staskawicz BJ. 2020. Structure of the activated ROQ1 resistosome directly recognizing the pathogen effector XopQ. *Science* 370: eabd9993.
- Mikami M, Toki S, Endo M. 2015. Comparison of CRISPR/Cas9 expression constructs for efficient targeted mutagenesis in rice. *Plant Molecular Biology* 88: 561–572.
- Moscou MJ, Bogdanov AJ. 2009. A simple cipher governs DNA recognition by TAL effectors. *Science* 326: 1501.
- Nakagawa T, Kurose T, Hino T, Tanaka K, Kawamukai M, Niwa Y, Toyooka K, Matsuoka K, Jinbo T, Kimura T. 2007. Development of series of gateway binary vectors, pGWBs, for realizing efficient construction of fusion genes for plant transformation. *Journal of Bioscience and Bioengineering* 104: 34–41.
- Naseem M, Kunz M, Dandekar T. 2017. Plant–pathogen maneuvering over apoplastic sugars. *Trends in Plant Science* 22: 740–743.
- Ochiai H, Inoue Y, Takeya M, Sasaki A, Kaku H. 2005. Genome sequence of *Xanthomonas oryzae* pv *oryzae* suggests contribution of large numbers of effector genes and insertion sequences to its race diversity. *Japan Agricultural Research Quarterly* 39: 275–287.
- Ogawa T, Morinaka T, Fujii K, Kimura T. 1978. Inheritance of resistance of rice varieties Kogyoku and Java 14 to bacterial group V of *Xanthomonas oryzae*. *Annals of the Phytopathological Society of Japan* 44: 137–141.
- Oliva R, Ji C, Atienza-Grande G, Huguet-Tapia JC, Perez-Quintero A, Li T, Eom JS, Li C, Nguyen H, Liu B *et al.* 2019. Broad-spectrum resistance to bacterial blight in rice using genome editing. *Nature Biotechnology* 37: 1344–1350.
- Paulus JK, van der Hoorn RAL. 2018. Tricked or trapped-two decoy mechanisms in host–pathogen interactions. *PLoS Pathogens* 14: e1006761.
- Read AC, Moscou MJ, Zimin AV, Perrea G, Meyer RS, Purugganan MD, Leach JE, Triplett LR, Salzberg SL, Bogdanov AJ. 2020. Genome assembly and characterization of a complex zBED-NLR gene-containing disease resistance locus in Carolina Gold Select rice with Nanopore sequencing. *PLoS Genetics* 16: e1008571.
- Read AC, Rinaldi FC, Hutin M, He YQ, Triplett LR, Bogdanov AJ. 2016. Suppression of *Xo1*-mediated disease resistance in rice by a truncated, non-DNA-binding TAL effector of *Xanthomonas oryzae*. *Frontiers in Plant Science* 7: 1516.
- Sharoni AM, Nuruzzaman M, Satoh K, Shimizu T, Kondoh H, Sasaya T, Choi IR, Omura T, Kikuchi S. 2011. Gene structures, classification and expression models of the AP2/EREBP transcription factor family in rice. *Plant and Cell Physiology* 52: 344–360.
- Sun J, Nishiyama T, Shimizu K, Kadota K. 2013. tcc: an R package for comparing tag count data with robust normalization strategies. *BMC Bioinformatics* 14: 219.
- Taoka KI, Shimatani Z, Yamaguchi K, Ogawa M, Saitoh H, Ikeda Y, Akashi H, Terada R, Kawasaki T, Tsuji H. 2021. Novel assays to monitor gene expression and protein–protein interactions in rice using the bioluminescent protein, NanoLuc. *Plant Biotechnology* 38: 89–99.
- Tian D, Wang J, Zeng X, Gu K, Qiu C, Yang X, Zhou Z, Goh M, Luo Y, Murata-Hori M *et al.* 2014. The rice TAL effector-dependent resistance protein XA10 triggers cell death and calcium depletion in the endoplasmic reticulum. *Plant Cell* 26: 497–515.
- Uji Y, Taniguchi S, Tamaoki D, Shishido H, Akimitsu K, Gomi K. 2016. Overexpression of OsMYC2 results in the up-regulation of early JA-responsive genes and bacterial blight resistance in rice. *Plant and Cell Physiology* 57: 1814–1827.
- Wamaita MJ, Yamamoto R, Wong HL, Kawasaki T, Kawano Y, Shimamoto K. 2012. OsRap2.6 transcription factor contributes to rice innate immunity through its interaction with receptor for activated kinase-C 1 (RACK1). *Rice* 5: 35.
- Wan L, Essuman K, Anderson RG, Sasaki Y, Monteiro F, Chung EH, Osborne Nishimura E, DiAntonio A, Milbrandt J, Dangel JL *et al.* 2019. TIR domains of plant immune receptors are NAD<sup>+</sup>-cleaving enzymes that promote cell death. *Science* 365: 799–803.
- Wang J, Hu M, Wang J, Qi J, Han Z, Wang G, Qi Y, Wang HW, Zhou JM, Chai J. 2019. Reconstitution and structure of a plant NLR resistosome conferring immunity. *Science* 364: eaav5870.
- Xie Z, Nolan TM, Jiang H, Yin Y. 2019. AP2/ERF transcription factor regulatory networks in hormone and abiotic stress responses in Arabidopsis. *Frontiers in Plant Science* 10: 228.
- Xu X, Xu Z, Ma W, Haq F, Li Y, Shah SMA, Zhu B, Zhu C, Zou L, Chen G. 2021. TALE-triggered and iTALE-suppressed Xa1 resistance to bacterial blight is independent of OsTFIIAγ1 or OsTFIIAγ5 in rice. *Journal of Experimental Botany* 72: 3249–3262.
- Yamaguchi K, Yamada K, Ishikawa K, Yoshimura S, Hayashi N, Uchihashi K, Ishihama N, Kishi-Kaboshi M, Takahashi A, Tsuge S *et al.* 2013. A receptor-like cytoplasmic kinase targeted by a plant pathogen effector is directly phosphorylated by the chitin receptor and mediates rice immunity. *Cell Host & Microbe* 13: 347–357.
- Yoshihisa A, Yoshimura S, Shimizu M, Yamaguchi K, Kawasaki T. 2021. Identification of TAL and iTAL effectors in the Japanese strain T7133 of *Xanthomonas oryzae* pv *oryzae*. *Journal of General Plant Pathology* 87: 354–360.
- Yoshimura S, Yamanouchi U, Katayose Y, Toki S, Wang ZX, Kono I, Kurata N, Yano M, Iwata N, Sasaki T. 1998. Expression of *Xa1*, a bacterial blight-resistance gene in rice, is induced by bacterial inoculation. *Proceedings of the National Academy of Sciences, USA* 95: 1663–1668.
- Yu D, Song W, Tan EYJ, Liu L, Cao Y, Jirschtzka J, Li E, Logemann E, Xu C, Huang S *et al.* 2022. TIR domains of plant immune receptors are 2',3'-cAMP/ cGMP synthetases mediating cell death. *Cell* 185: 2370–2386.
- Zhang B, Zhang H, Li F, Quyang Y, Yuan M, Li X, Xiao J, Wang S. 2020. Multiple alleles encoding atypical NLRs with unique central tandem repeats in rice confer resistance to *Xanthomonas oryzae* pv *oryzae*. *Plant Communications* 1: 100088.
- Zuluaga P, Szurek B, Koebnik R, Kroj T, Morel JB. 2017. Effector mimics and integrated decoys, the never-ending arms race between Rice and *Xanthomonas oryzae*. *Frontiers in Plant Science* 8: 431.

## Supporting Information

Additional Supporting Information may be found online in the Supporting Information section at the end of the article.

**Fig. S1** Western blot analysis of green fluorescence protein-fused Xa1 and its truncated proteins for the experiment shown in Fig. 1(b).

**Fig. S2** Alignment of the amino acid sequences in the N- and C-terminal regions of Xoo1132 and AvrXa7.

**Fig. S3** Western blot analysis of green fluorescence protein-fused AvrXa7, Xoo1132, Xoo1132<sup>1–277</sup> and Xoo1132<sup>871–1002</sup> for the experiments shown in Fig. 1(e).

**Fig. S4** Western blot analysis of the Xa1 and transcription activator-like effector proteins for the bimolecular fluorescence complementation experiments shown in Fig. 2(a).

**Fig. S5** Western blot analysis of LgBiT-fused Xa1<sup>1–325</sup> protein and SmBiT-fused transcription activator-like effectors in split NanoLuc luciferase assays for the experiments shown in Fig. 2(b,c).

**Fig. S6** Interaction of Xa1<sup>1–325</sup> with Xoo1132 and AvrXa7.

**Fig. S7** Western blot analysis of the Xa1-truncated proteins and the OsERF101 protein for the two-hybrid assay shown in Fig. 3 (a).

**Fig. S8** Western blot analysis of the proteins expressed in rice protoplasts for the experiments shown in Fig. 3(b–e).

**Fig. S9** Western blot analysis of OsERF101, Xa1<sup>1–325</sup> and the transcription activator-like effectors for the two-hybrid assay shown in Fig. 3(f).

**Fig. S10** The BED domain of Xa1 interacts with the transcription activator-like effectors in *OsERF101-OX* and *oserf101* cells.

**Fig. S11** Yeast three-hybrid assay showing the lack of interaction between the BED domain and the transcription activator-like effectors in the presence of OsERF101.

**Fig. S12** The mutations produced in this study.

**Fig. S13** Transcript levels of *OsERF101* in leaves of the transgenic plants overexpressing *OsERF101*.

**Fig. S14** Cell death assays using a DEX-inducible AvrXa7 system.

**Fig. S15** Blast resistance of *OsERF101-OX* and *oserf101* plants.

**Fig. S16** Cell death responses induced by transient expression of *Xa10*.

**Fig. S17** *Cis* regulatory elements enriched in genes downregulated in *OsERF101-OX* plants.

**Fig. S18** *Cis* regulatory elements enriched in genes downregulated in *oserf101* plants.

**Table S1** Primers used in this study.

**Table S2** Candidate Xa1 interactors.

**Table S3** Differentially expressed gene list and annotations.

**Table S4** Gene Ontology enrichment analysis of the differentially expressed genes.

**Table S5** List of genes identified by clustering analysis.

Please note: Wiley Blackwell are not responsible for the content or functionality of any Supporting Information supplied by the authors. Any queries (other than missing material) should be directed to the *New Phytologist* Central Office.